

FILE COPY

*Bookcase*

# Microwave Breakdown of a Gas in a Cylindrical Cavity of Arbitrary Length

MELVIN A. HERLIN, SANBORN C. BROWN

TECHNICAL REPORT NO. 77

JULY 30, 1948

RESEARCH LABORATORY OF ELECTRONICS  
MASSACHUSETTS INSTITUTE OF TECHNOLOGY

The research reported in this document was made possible through support extended the Massachusetts Institute of Technology, Research Laboratory of Electronics, jointly by the Army Signal Corps, the Navy Department (Office of Naval Research), and the Air Force (Air Materiel Command), under the Signal Corps No. W-36-039 sc-32037.

MASSACHUSETTS INSTITUTE OF TECHNOLOGY  
Research Laboratory of Electronics

Technical Report No. 77

July 30, 1948

MICROWAVE BREAKDOWN OF A GAS IN A CYLINDRICAL CAVITY  
OF ARBITRARY LENGTH

Melvin A. Herlin, Sanborn C. Brown

Abstract

It is possible to consider breakdown in a cylindrical microwave cavity whose radius is large compared to its length as approaching the conditions of parallel-plate breakdown. This assumption has been used to measure high-frequency ionization coefficients. The present paper investigates the corrections to be made when the length is increased. Numerical results are given for cavities whose ratios of radius to length are as low as 0.5, and the method is applicable to any cylindrical cavity. The breakdown data in these longer cavities are used to extend the high-frequency ionization coefficient curves for air by a factor of ten.



MICROWAVE BREAKDOWN OF A GAS IN A CYLINDRICAL CAVITY  
OF ARBITRARY LENGTH

The electrical breakdown of a gas at microwave frequencies has been discussed in two papers by the authors. The first<sup>1</sup> developed the principle of balancing the generation of electrons through ionization by collision against the loss of electrons through diffusion. The resulting breakdown criterion appeared as the solution of a characteristic-value problem. A new ionization coefficient appropriate to the high-frequency conditions was introduced. It is necessary to know this quantity as a function of the experimental conditions in order to compute the electric field for breakdown. Breakdown data were used to give experimental values of the ionization coefficient. The second paper<sup>2</sup> illustrated a computing technique for solving the boundary-value problem for breakdown between coaxial cylinders. Comparison with experiment indicated that the breakdown theory is valid.

The present paper develops the breakdown criterion for the case of the  $TM_{010}$ -mode cylindrical cavity. The object of this computation is primarily to extend the range of the experimental data for the ionization coefficient beyond the region where the cavity height is small compared to its diameter. This generalization removes the assumption that the cavity approximates the conditions of infinite parallel plates. Moreover, a theory for breakdown in this cavity is valuable in itself, because the cavity is commonly used in microwave work.

1. Breakdown Theory

The differential equation and boundary condition which lead to the breakdown field strength are obtained from the continuity requirement on the electrons. The resulting differential equation is

$$\nabla^2 \psi + \xi E^2 \psi = 0, \quad (1)$$

where the electron diffusion current density potential  $\psi$  is given by

$$\psi = Dn,$$

- 
1. M. A. Herlin and S. C. Brown, RLE Technical Report No. 60; also Phys. Rev. 74, 291 (1948).
  2. M. A. Herlin and S. C. Brown, RLE Technical Report No. 72; also Phys. Rev. 74, 910 (1948).

and  $\zeta$  is the high-frequency ionization coefficient defined by

$$\zeta = \nu / DE^2.$$

The quantity  $n$  is the electron density function;  $D$  is the electronic diffusion coefficient;  $\nu$  is the net production rate of electrons per electron; and  $E$  is the rms value of the electric field intensity. The boundary condition that  $\psi$  be zero on the walls of the discharge cavity is sufficiently accurate. The ionization coefficient is a function of  $E/p$  and  $p\lambda$ , where  $E/p$  expresses the energy gained by an electron per collision at zero frequency, and  $p\lambda$  expresses the ratio of the collision frequency of the electrons to the frequency of the applied high-frequency field. The quantity  $p$  is the pressure and  $\lambda$  is the free-space wavelength of the electric field. The electric field appears explicitly in Eq. (1) because it varies with position in the cavity. On the other hand,  $p\lambda$  is constant throughout the cavity. The electric field in an arbitrary cavity is given in the form

$$E = E_0 f(x, y, z),$$

where  $E_0$  is the maximum value of the electric field and  $f$  is a geometrical factor obtained from a solution for the field distribution within the cavity as an electromagnetic boundary-value problem. The value of  $f$  is unity at the maximum-field point. The degree of excitation of the cavity is expressed by  $E_0$ , and the relative field distribution through the cavity is independent of the excitation. The boundary-value problem of finding a non-zero solution to Eq. (1) with the boundary condition that  $\psi$  be zero on the cavity walls, leads to a characteristic value of  $E_0$ , which is the breakdown field at the maximum-field point.

Integration of Eq. (1) is simplified by the use of an approximation to the ionization coefficient which was used in the analysis of the coaxial cylinder.<sup>1</sup> This approximation expresses the ionization coefficient as the simple analytic function,

$$\zeta = \zeta_0 \left(\frac{E}{E_0}\right)^{\beta-2} = \left(\frac{k}{E_0}\right)^2 \left(\frac{E}{E_0}\right)^{\beta-2} \quad (2)$$

where  $\zeta_0$  is the value of the ionization coefficient at the maximum-field point. The quantity  $k$  is introduced for mathematical convenience in the following equations. It has the dimensions of reciprocal length, and appears multiplied into the radius variable below. The quantity  $(\beta-2)$  is obtained as the slope of the  $\zeta$  versus  $E/p$  plot on a logarithmic scale at the point  $E_0/p$ . This approximation gives accurate results because it is correct where the ionization is high, and is inaccurate only where the ionization is low and

---

1. See footnote 2, p. 1.

therefore has little effect on the solution of the equation.

The electric field in the  $TM_{010}$ -mode cylindrical cavity, shown in Fig. 1, is given by the expression,

$$E = E_0 J_0(2.405r/R). \quad (3)$$

It depends on the radial coordinate only, which allows the differential equation, Eq. (1) to separate. Separation results in

$$\psi = A \sin \frac{\pi z}{L} \phi(r),$$

where A is a constant, L is the length of the cylindrical cavity, z is the axial coordinate, and  $\phi$  is a function only of r, determined from the differential equation

$$\frac{1}{r} \frac{d}{dr} \left( r \frac{d\phi}{dr} \right) + \left( \zeta E^2 - \frac{\pi^2}{L^2} \right) \phi = 0. \quad (4)$$

The approximation of Eq. (2) and the electric field of Eq. (3) substituted into Eq. (4) lead to the equation

$$\frac{1}{r} \frac{d}{dr} \left( r \frac{d\phi}{dr} \right) + \left[ k^2 J_0^2(2.405r/R) - \frac{\pi^2}{L^2} \right] \phi = 0. \quad (5)$$

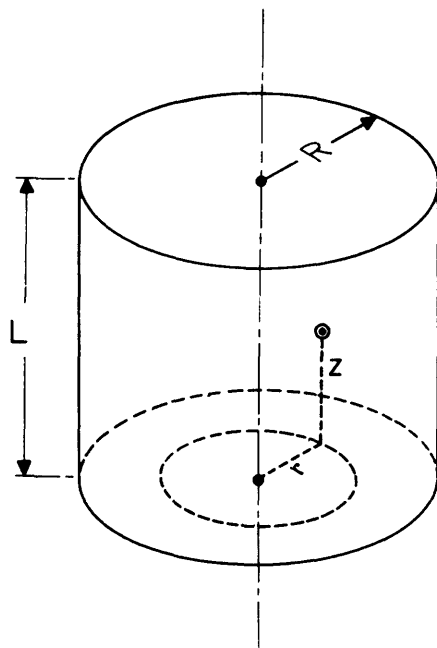


Fig. 1. Cylindrical cavity, showing coordinates and dimensions. The electric field is given by Eq. (3) for the  $TM_{010}$ -mode of oscillation.

It is difficult to find an analytic solution to this equation. A good approximation is to express the Bessel function as the first two terms of its power series. This approximation is also accurate where the ionization is high and fails only where it is low. Equation (5) then becomes

$$\frac{1}{r} \frac{d}{dr} \left( r \frac{d\phi}{dr} \right) + \left[ k^2 \left( 1 - \frac{r^2}{b^2} \right) - \frac{\pi^2}{L^2} \right] \phi = 0, \quad (6)$$

where

$$b = 0.831 R / \sqrt{\beta} \quad (7)$$

is the radius at which the ionization goes to zero under the above assumptions.

The ionization function in Eq. (6) is negative beyond  $r = b$ ; this is not physically correct. Accordingly, the ionization is set equal to zero from  $r = b$  to  $r = R$ . Equation (6) is used in the range  $0 \leq r \leq b$ , and in the range  $b \leq r \leq R$  the equation

$$\frac{1}{r} \frac{d}{dr} \left( r \frac{d\phi}{dr} \right) - \frac{\pi^2}{L^2} \phi = 0 \quad (8)$$

is applied. The ionization function employed here is compared with the actual ionization function in Fig. 2. They are identical near  $r = 0$ , where the ionization is high. The error in the approximation becomes positive as

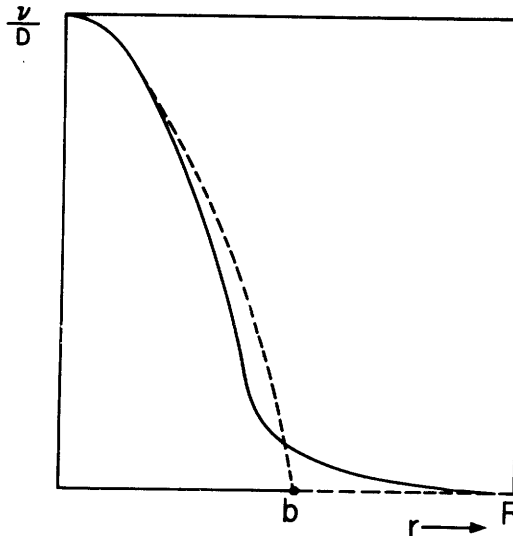


Fig. 2. Comparison of actual ionization function (solid curve) with its approximation (dotted curve).

r increases, and negative as it approaches the radius b. Beyond r = b, the ionization drops rapidly to zero and is approximated by the value zero. The boundary condition on  $\phi$  is that it be zero at r = R and that its derivatives and value match at r = b.

Letting the ionization be zero beyond the radius b neglects the effect of attachment in this region, since attachment contributes a negative term to the net production rate of electrons. However, attachment is properly accounted for within the radius b, where the breakdown is influenced most heavily. Neglecting attachment outside the radius b is the same kind of approximation as letting the ionization function be represented by a poor approximation in the low-field region, which is known to introduce very little error. This statement holds if the negative production rate in the low-field region is small in magnitude compared to the positive production rate in the large-field region, which must be the case for breakdown to occur.

The solution of Eq. (6) is

$$\phi = e^{-\frac{\sigma x^2}{2}} M\left(\frac{2\sigma}{4\sigma} - 1, 1, \sigma x^2\right), \quad (9)$$

where

$$\sigma = \frac{1}{kb\left(1 - \frac{\pi^2}{k^2 L^2}\right)},$$

$$x = \sqrt{1 - \frac{\pi^2}{k^2 L^2}} kr,$$

and M is the confluent hypergeometric function.<sup>1</sup> The second solution is omitted because it has a singularity at the origin. The solution of Eq. (8) is

$$\phi = iH_0^{(1)}(i\pi r/L) - KJ_0(i\pi r/L). \quad (10)$$

where K is a constant of integration. It is chosen to make  $\phi$  equal to zero at the point r = R, and it is thus a function of the ratio R/L.

The Bessel function  $J_0$  in Eq. (10) is an exponentially increasing function of r, while the Hankel function  $H_0^{(1)}$  is an exponentially decreasing

---

1. The confluent hypergeometric function is defined as in E. Jahnke and F. Emde, "Funktionentafeln", B. G. Teubner, Leipzig and Berlin, 1933, p 275.

function of  $r$ . Therefore,  $\kappa$  is zero when  $R/L$  is infinity. The exponential decrease in electron density in the region where the ionization rate is very small, and assumed to be zero, is a result of diffusion to the end plates of the cavity. If  $R/L$  is not infinite, the negative exponentially increasing Bessel function term provides the extra decrease in electron density which causes it to go to zero at the finite cavity radius. Numerical computation of the relative magnitudes of these two terms shows, however, that for a wide range of the ratio  $R/L$ , the value of  $\kappa$  is very small and the contribution from the Bessel function term is correspondingly negligible. Thus, for  $R/L$  greater than 0.5, the Bessel term may be neglected. The range below 0.5 may be computed if the Bessel term is retained. The numerical computations were performed only for  $R/L > 0.5$ , so that the results presented here are applicable to cavities whose heights are smaller than their diameters. This increase in the coverage of the range of  $R/L$  is a substantial gain over the coverage of the parallel-plate treatment, for which  $R/L$  should be greater than 15.

The solutions given in Eqs. (9) and (10) should each be written with another constant of integration which appears as a multiplying constant. This constant is not written because the matching condition may be satisfied by making the ratio  $\frac{d\phi}{dr}/\phi$  equal on both sides of the matching point  $r = b$ . The multiplying constant cancels in the ratio. The resulting equation is a transcendental equation for the breakdown field:

$$x_0 \frac{H_1^{(1)}(ix_0)}{iH_0^{(1)}(ix_0)} = y_0 \left[ \frac{2\sigma - 1}{2\sigma} \frac{M\left(\frac{6\sigma - 1}{4\sigma}, 2, y_0\right)}{M\left(\frac{2\sigma - 1}{4\sigma}, 1, y_0\right)} - 1 \right], \quad (11)$$

where

$$x_0 = \pi b/L ;$$

$$y_0 = kb .$$

Equation (11) may be solved for  $kb$  as a function of  $kL$ . The results are most conveniently expressed by expressing  $(\pi/kL)^2$  as a function of  $b/L$ . This plot is shown in Fig. 3. Parallel-plate breakdown requires that  $k = \pi/L$ , so that the ordinate approaches unity for large  $b/L$ . If the tube is long or the slope of the ionization coefficient curve is large,  $b/L$  is small and a larger value of  $k$ , and therefore electric field, is required

for breakdown, relative to what would be required with a uniform field. Figure 3 may be regarded as expressing an equivalent parallel-plate separation to give the same breakdown field as that of the actual cavity.

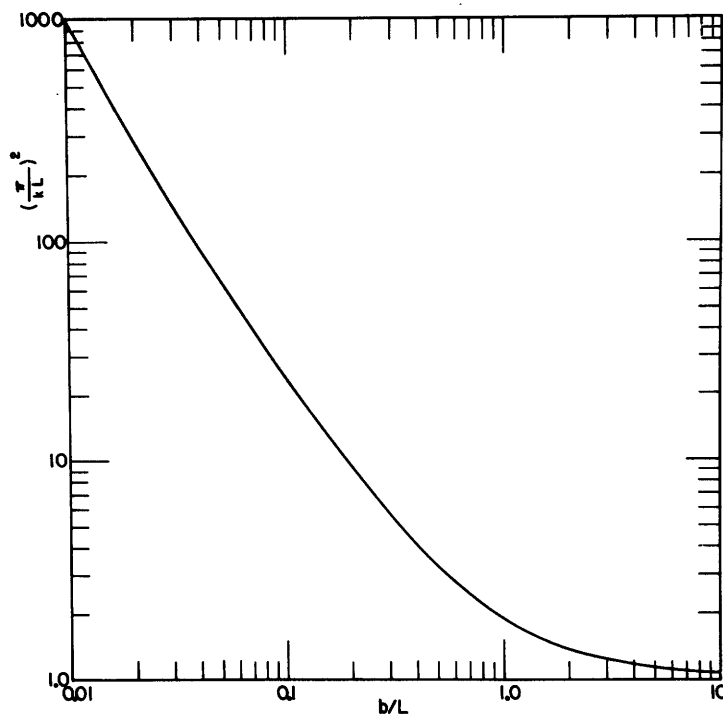


Fig. 3. Solution of the transcendental breakdown equation, Eq. (11). The ordinate is the square of the ratio of the equivalent infinite parallel-plate separation to the real cavity length.

## 2. Application to Extending the Ionization Coefficient Curves

These results may be used for computing breakdown fields in the  $TM_{010}$ -mode cylindrical cavity from the curves giving the ionization coefficient as a function of the experimental parameters. They are used in this paper, however, to extend the range of experimental values of the ionization coefficient from experimental breakdown data in longer cavities than are permitted by the uniform-field theory.<sup>1</sup> The procedure is as follows: The first approximation to the ionization coefficient curves is computed by assuming a uniform field. The various constant  $p\lambda$  curves are drawn through the appropriate points. The slopes of these preliminary curves then lead, with the aid of Fig. 3, to correction factors which provide the second approximation to the ionization coefficient curves. The process is repeated until no further correction is indicated.

Results on air in two cavities resonant at 9.6-cm wavelength are shown in Figs. 4 and 5. Breakdown fields,  $E$  volts/cm (rms), were measured

1. See footnote 1. p.1.

by increasing the magnetron power gradually until the transmitted power from the cavity dropped suddenly, the sudden drop indicating breakdown. The field was computed from the measured breakdown power and cavity parameters.

Figure 4, computed from experimental E-versus-p curves, shows the quantity  $(\pi/EL)^2$  as a function of E/p for various cavity lengths. The diameters were

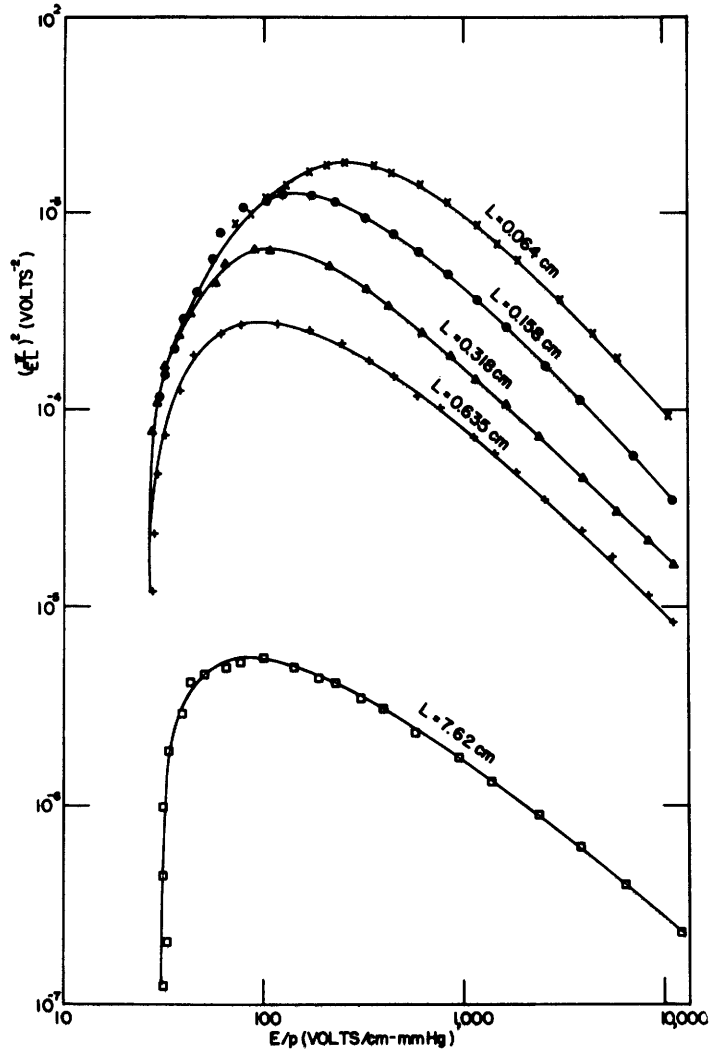


Fig. 4. Experimental values of  $(\pi/EL)^2$  as a function of E/p for various cavity lengths, obtained from data of breakdown-field E versus pressure p. The ordinate would be the high-frequency ionization coefficient if the experiment were performed between infinite parallel plates.

all the same and equal to that necessary to give a resonant wavelength of 9.6 cm. If the field were uniform,  $(\pi/EL)^2$  would be equal to the high-frequency ionization coefficient. However, the non-uniformity must be taken into account, especially for the long cavity whose curve appears at

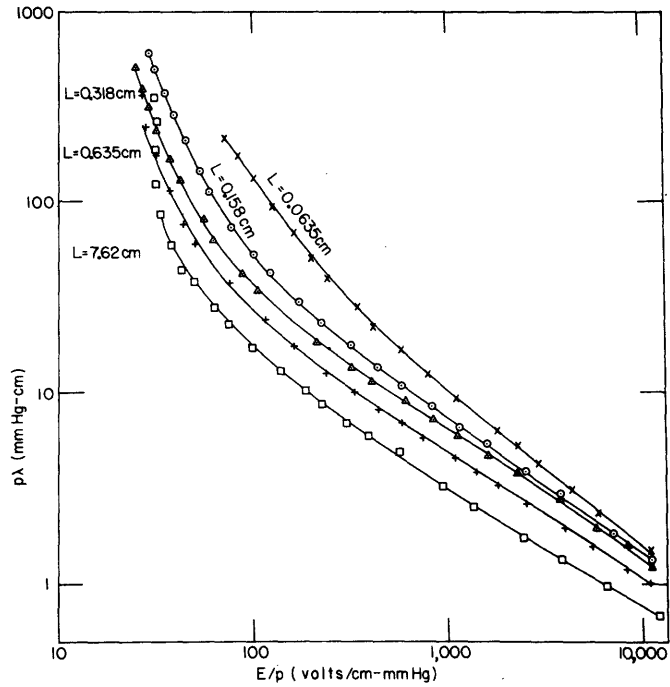


Fig. 5. Curves of  $p\lambda$  versus  $E/p$  for various cavity lengths. These curves are used to obtain constant  $p\lambda$  curves of Fig. 6.

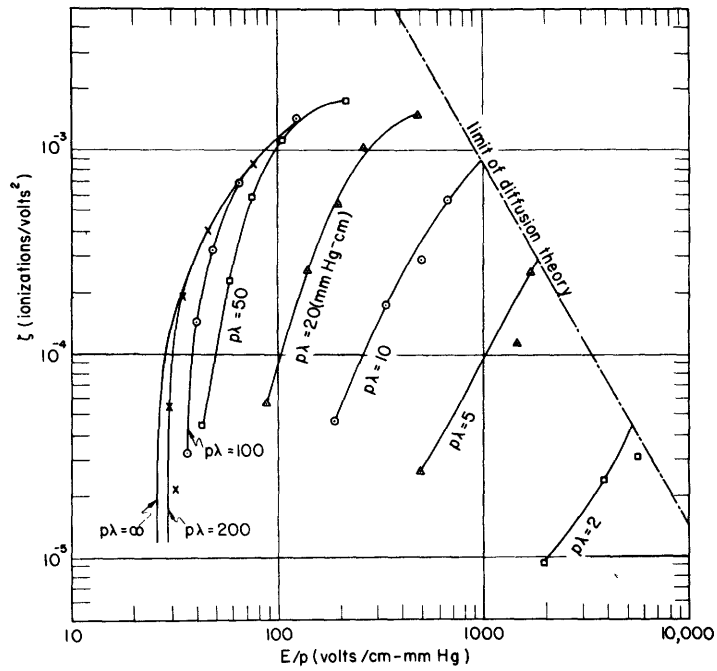


Fig. 6. Ionization coefficient as a function of  $E/p$  and  $p\lambda$ , obtained from correction of curves of Fig. 4 by using Fig. 3.

Table I. Values of the Ionization Coefficient  $\zeta$  for Air.

E/p	$p\lambda$									
	$\infty$	200	100	50	20	10	5	2		
26	$1.2 \times 10^{-5}$									
27	$4.5 \times 10^{-5}$									
29	$1.1 \times 10^{-4}$	$1.2 \times 10^{-5}$								
30	$1.3 \times 10^{-4}$	$5.7 \times 10^{-5}$								
36	$2.2 \times 10^{-4}$	$2.1 \times 10^{-4}$	$3.5 \times 10^{-5}$							
40	$3.0 \times 10^{-4}$	$3.0 \times 10^{-4}$	$1.5 \times 10^{-4}$							
45	$3.9 \times 10^{-4}$	$3.9 \times 10^{-4}$	$2.5 \times 10^{-4}$	$5.8 \times 10^{-5}$						
50	$4.8 \times 10^{-4}$	$4.8 \times 10^{-4}$	$3.6 \times 10^{-4}$	$1.0 \times 10^{-4}$						
60	$6.4 \times 10^{-4}$	$6.4 \times 10^{-4}$	$5.9 \times 10^{-4}$	$2.5 \times 10^{-4}$						
70	$7.8 \times 10^{-4}$	$7.8 \times 10^{-4}$	$7.8 \times 10^{-4}$	$4.8 \times 10^{-4}$						
90	$1.04 \times 10^{-3}$	$1.04 \times 10^{-3}$	$1.04 \times 10^{-3}$	$8.9 \times 10^{-4}$	$6.2 \times 10^{-5}$					
110	$1.24 \times 10^{-3}$	$1.24 \times 10^{-3}$	$1.24 \times 10^{-3}$	$1.2 \times 10^{-3}$	$1.2 \times 10^{-4}$					
140	$1.5 \times 10^{-3}$	$1.5 \times 10^{-3}$	$1.5 \times 10^{-3}$	$1.5 \times 10^{-3}$	$2.6 \times 10^{-4}$					
190	$1.75 \times 10^{-3}$	$1.75 \times 10^{-3}$	$1.75 \times 10^{-3}$	$1.75 \times 10^{-3}$	$5.5 \times 10^{-4}$	$4.9 \times 10^{-5}$				
250					$8.9 \times 10^{-4}$	$9.2 \times 10^{-5}$				
350					$1.3 \times 10^{-3}$	$1.85 \times 10^{-4}$				
500					$1.54 \times 10^{-3}$	$3.6 \times 10^{-4}$	$2.7 \times 10^{-5}$			
700						$5.9 \times 10^{-4}$	$5.0 \times 10^{-5}$			
1000						$9.0 \times 10^{-4}$	$9.5 \times 10^{-5}$			
2000							$3.4 \times 10^{-4}$	$9.5 \times 10^{-6}$		
3500								$2.0 \times 10^{-5}$		
5500								$4.6 \times 10^{-5}$		

the bottom of the figure. Figure 5 shows  $p\lambda$  plotted as a function of  $E/p$ . The values of  $E/p$  for various constant  $p\lambda$  values may be transferred to Fig. 4 and the constant  $p\lambda$  curves drawn in. (These curves are not shown in Fig. 4 to avoid confusing the diagram.) The curves are then corrected as described in the previous paragraph to yield the final set of ionization coefficient curves of Fig. 6. A curve connecting the bottom set of points in Fig. 6 is the corrected version of the lowest curve of Fig. 4. The line showing the limit of diffusion theory is where the mean free path is of the order of the tube size. The data of Fig. 6 represent a complete measurement of the ionization coefficient for air, and is therefore given in detail in Table I.

### 3. Discussion

The constant  $p\lambda$  curves agree with the curves given in another report<sup>1</sup> with two exceptions. At low  $E/p$ , and high  $p\lambda$ , the curves drop more steeply than expected from the previous results. A possible reason is that attachment balances ionization at a value of  $E/p$  of the order of 30, and this balance is very sensitive to uncontrolled impurities in the air. When this value of  $E/p$  is exceeded slightly, the curves agree until the low values of  $p\lambda$  at the high  $E/p$  end are reached. There the new data give curves of smaller slope than those shown in the previously mentioned report.<sup>2</sup> The former data are very near the region where the diffusion theory fails because the mean free path is of the order of the cavity dimensions, and were given tentatively until the range could be extended.

This paper has given a method of treating the effect of the non-uniform field in the  $TM_{010}$ -mode cylindrical cavity. With the high-frequency ionization coefficient known, the breakdown field can be computed from the theory. Experimental values of the breakdown field were used to extend the range of the ionization coefficient curves for air by a factor of ten. This extension of the breakdown theory to cylindrical cavities, which has been illustrated by results for air, is generally applicable to all gases.

---

1. See footnote 1, p.1.  
2. Ibid

